



# Biodiesel production from transesterification of Australian *Brassica napus* L. oil: optimisation and reaction kinetic model development

M. A. Hazrat<sup>1</sup> · M. G. Rasul<sup>1</sup> · M. M. K. Khan<sup>2</sup> · N. Ashwath<sup>3</sup> · I. M. R. Fattah<sup>4,5</sup>  · Hwai Chyuan Ong<sup>6</sup> · T. M. I. Mahlia<sup>7</sup>

Received: 18 September 2021 / Accepted: 8 June 2022 / Published online: 28 July 2022  
© The Author(s) 2022

## Abstract

Edible oil-based feedstocks based biodiesel is still leading the industry around the world. Canola oil (*Brassica napus* L.) contributes significantly to that race. Process optimisation and the development of reaction kinetic models of edible oil feedstocks are still required since the knowledge of kinetics is needed for designing industrial facilities and evaluating the performance of catalysts during transesterification or other related processes in a biorefinery. This research focuses on the transesterification process for biodiesel production because of its higher output efficiency, reactivity with feedstock, techno-economic feasibility in terms of FFA content, and environmental sustainability. The response surface method with the Box–Behnken model was used to optimise the process. Multivariate analysis of variance (ANOVA) was also performed to investigate the effectiveness of the regression model. The optimal process conditions were found to be 5.89 M methanol, 0.5% (w/w) KOH, 60 °C and 120 min. The predicted yield was 99.5% for a 95% confidence interval (99.1, 99.9). The experimental yield was 99.6% for these conditions. Two different kinetic models were also developed in this study. The activation energy was 16.9% higher for the pseudo-first-order irreversible reaction than for the pseudo-homogenous irreversible reaction. Such a comprehensive analysis will assist stakeholders in evaluating the technology for industrial development in biodiesel fuel commercialisation.

**Keywords** Transesterification · Homogeneous alkaline catalyst · RSM · Optimisation · Reaction kinetics · Biodiesel

## Abbreviations

CB	Canola oil biodiesel
ANOVA	Analysis of variance
FFA	Free fatty acid
RSM	Response surface methodology

---

✉ M. A. Hazrat  
alihazrat20@gmail.com

✉ I. M. R. Fattah  
IslamMdRizwanul.Fattah@uts.edu.au

BB	Box Behnken
HEAR	High erucic acid rapeseed oil
ANFIS	Adaptive neuro-fuzzy inference system
NaOH	Sodium hydroxide
FAME	Fatty acid methyl ester
KOH	Potassium hydroxide
ANN	Artificial neural network
GWO	Grey wolf optimiser
VIF	Variables of inflation factors

## 1 Introduction

Biodiesel has been regarded as a sustainable fuel alternative for diesel fuel owing to its capacity to biodegrade, non-polluting to water and land, lack of aromatic and sulphur constituents, improved lubricity benefits, storage, transport, and safe handling (Fattah et al., 2020; Hoang et al., 2021; Su et al., 2021). This can be produced from various types of edible or inedible feedstocks, waste animal fat, waste cooking oil, algae, and biomass (Ong et al., 2020; Singh et al., 2020). Based on scientific evolution on feedstock diversification for fuel production, the commonly used biofuel feedstocks have been classified as first-generation (oils from edible feedstocks), second-generation (fuel derived from inedible sources such as lignocellulose, animal fat, and inedible crops), third-generation (microalgae), and fourth-generation (feedstocks capable of absorbing CO<sub>2</sub> and containing higher lipid and energy values) (Ampah et al., 2022; Mofijur et al., 2014; Singh et al., 2020). Mainly regional availability of feedstocks, land capacity and technology influence the selection of feedstocks to be used for biodiesel. Although first-generation feedstocks are primary raw materials for biodiesel production, the "food versus fuel" debate and land availability issue in many countries have influenced the production of biodiesel from inedible feedstocks in addition to the improvement of biodiesel production technologies (Fattah et al., 2014; Imtenan et al., 2014; Milledge et al., 2014; Ramos et al., 2019). Among the feedstocks used for total global biodiesel production (about 41.2 million tonnes), the overall share of biodiesel produced from palm oil (35%), soybean oil (26%), rapeseed oil (16%), waste cooking oil (10%), animal fat (7%) and other feedstocks shared about 6% (Union Zur Förderung Von Oel- Und Proteinpflanzen E.V. (UFOP), 2020a). Indeed, only 5% of the total global oilseeds and 9% of the total global production of grains were used for biodiesel and bioethanol production in the year 2018–2019 (UFOP, 2020b). The amount of erucic acid (C22:1) in the rapeseed oil determines whether it is suitable for industrial use or human consumption (less than 2%), and the feedstocks are included in the family Cruciferae (Agriculture and Horticulture Development Board (AHDB), 2020a; Gunstone & Harwood, 2007). Rapeseed oils are categorised based on their content of erucic acid. The lower percentage of erucic acid (<2%) containing rapeseed oil is commonly known as "canola oil", which is edible to humans (AHDB, 2020b; Warner & Lewis, 2019). In the European Union, the erucic acid content for edible rapeseed oil has been limited to up to 5%, and it is known as "Rapeseed 00" (AHDB, 2020b; Warner & Lewis, 2019). On the other hand, the commonly known high erucic acid rapeseed oil (HEAR), which is categorised as the inedible rapeseed oil, can contain as much as 45–60% of erucic acid (Warner & Lewis, 2019). Overall, about 71.91 million tonnes (Mt) of rapeseed oil (including canola oil and inedible rapeseed oil) were produced globally in the year 2018, and the top producers were Canada (20.34 Mt),

China (13.28 Mt), India (8.43 Mt), France (4.95 Mt) and Australia (3.9 Mt), respectively (Food and Agricultural Organization (FAO), 2019).

The fatty acid methyl ester (FAME) composition of the biodiesel governs both the physical and chemical properties of the biodiesel (Atique et al., 2022; Knothe, 2005). Although the composition may be changed, keeping almost the same quantity of long-chain saturated and monounsaturated fatty acid methyl esters in canola oil biodiesel (CB) would provide superior long-term storage stability, and cold flow characteristics retention, and kinematic viscosity (Kanca & Temur, 2016). Alkaline homogenous catalysts can be highly efficient in the conventional transesterification reaction to produce CB from canola oil (Bohlouli & Mahdavian, 2019; Ramos et al., 2019). Sodium hydroxide (NaOH) and potassium hydroxide (KOH) are the most commonly used alkaline homogenous catalysts, whereas methanol ( $\text{CH}_3\text{OH}$ ) is a primarily used reactant for transesterification reactions (Fattah et al., 2020; Khan et al., 2021). The determination of optimal operating parameters can be useful in investigating the economic benefit of the biodiesel production processes used from a feedstock (Ranjitha et al., 2020). Various modelling tools such as response surface methodology-artificial neural network (RSM-ANN), ANN-ant colony optimisation, RSM-Adaptive neuro-fuzzy inference system (ANFIS), and grey wolf optimiser (GWO) have been employed for modelling transesterification parameters for various types of oily feedstocks (Fayyazi et al., 2015; Kumar et al., 2017; Okwu et al., 2021; Samuel et al., 2020; Veza et al., 2022). Several recent studies have focussed on first-generation biodiesel feedstocks. For example, Encinar et al. (2022) carried out a kinetic study of homogeneous base and acid catalysts such as KOH, NaOH,  $\text{CH}_3\text{OK}$ ,  $\text{H}_2\text{SO}_4$ ,  $\text{H}_3\text{PO}_4$  and  $\text{CH}_3\text{C}_6\text{H}_4\text{SO}_3\text{H}$  utilised in the transesterification of soybean oil. They proposed a second-order kinetic model for base homogeneous catalytic transesterification, whereas a pseudo-first-order reaction was proposed in the case of methanol/oil ratios higher than 9:1. A pseudo-first-order reaction was proposed for homogeneous acid catalysis. In an earlier study, Encinar et al. (2018) reported that the transesterification of rapeseed oil using KOH as a catalyst and ultrasonic excitation as a heat source followed a pseudo-first-order kinetic model and the activation energy as 25.51 kJ/mol. Choudhury et al. (2014) carried out ultrasonic-assisted biodiesel synthesis using *Jatropha curcas* as feedstock and chlorosulfonic acid as catalyst (methanol as solvent). They reported that this process followed pseudo-first-order kinetic model and the activation energy of the process was 57.33 kJ/mol.

In this article, Australian grown canola oil (i.e. *Brassica napus* L.) was considered to determine the optimal biodiesel production parameters as well as the reaction kinetic model (Australian Export Grains Innovation Centre (AEGIC), 2017; Office of the Gene Technology Regulator (OGTR), 2018). Australia is one of the top canola oil producers in the world. Not all the produced canola oil is used as food; instead, a portion of it is used for industrial applications (AEGIC, 2017). It is essential to optimise the biodiesel production process for fuel production from this high-quality canola oil. The optimisation process was performed by following the response surface methodology (RSM), and the Box Behnken (BB) method was used to model the experimental variable parameters. RSM is an effective statistical approach that can model the issue based on supplied variables and analyse the responses to deliver a dependable, optimum solution that experimental designs can test with high accuracy (Montgomery, 2013; Samuel & Okwu, 2019; Singh et al., 2021). RSM offers the benefit of lowering the number of experimental runs required to provide statistically acceptable findings (Betiku & Ajala, 2014). This study focused on conventional transesterification process optimisation due to its higher yield efficiency, reactivity with feedstock, techno-economic feasibility in terms of FFA content, yield efficiency, and environmental sustainability, all of which are important factors to consider before deciding on

the type of feedstock. A kinetic model for a reaction process can predict similar reaction outputs with a variation of time and temperature if other parameters are kept constant, thus facilitating process design (Encinar et al., 2022). The study of kinetic parameters is particularly important for the correct implementation of this kind of process in real biorefineries, especially concerning reactor design and reagent supply.

## 2 Materials and methods

### 2.1 Materials

Refined canola oil (*Brassica napus* L.) was purchased from a local supermarket. Both methanol ( $\text{CH}_3\text{OH}$ ) and potassium hydroxide (KOH) were analytical grade chemicals (>99% purity). The batch reactor was equipped with a 3-neck round bottom thick-walled flask, a refluxing condenser, water bath, magnetic stirrer, and a heating system with feedback-controlled temperature and stirring speed controller. The reactor flask was half-submerged in the water bath in a glass beaker and clamped with stable stands to ensure better heat transfer to reactants.

### 2.2 Methods

#### 2.2.1 Transesterification of canola oil

In order to conduct the transesterification reaction of the canola oil, various steps were strictly followed to ensure efficient process output based on the designed process parameters. Before pouring the oil into the reactor, it was heated at 110 °C for 30 min in a wide-open glass beaker to remove moisture. Magnetic stirring (650 rpm) was performed to ensure better convective heat transfer and vaporisation of moisture. Then the oil was poured into the reactor flask after the oil temperature dropped below 50 °C. While oil temperature was maintained at the designed temperature range, the KOH catalyst was dissolved in  $\text{CH}_3\text{OH}$  by heating to (50 °C) and stirring in a separate beaker. When the KOH was totally dissolved in  $\text{CH}_3\text{OH}$ , the solution was poured into the reactor flask through one of the available necks and sealed with a glass stopper to allow the transesterification reaction to occur for the designed reaction period. Once the reaction was visibly completed, all the ingredients were poured into a separating funnel and allowed to settle down for more than 12 h. Glycerol was removed from the lower part of the funnel, and the rest of the FAME,  $\text{CH}_3\text{OH}$  and impurities were washed thoroughly with tap water to remove  $\text{CH}_3\text{OH}$ , soap and other impurities. When the visible water and FAME separating layer were observed, washing was concluded. Then the FAME was heated at 110 °C for an hour to remove any traces of water in the biodiesel. The drying process is important to maintain the limit of moisture content in biodiesel to meet either ASTM D6751 or EN14214 standards. After drying and cooling, the canola biodiesel (CB) or canola oil fatty acid methyl esters were obtained. FAME was centrifuged (Model: ThermoFisher D-37520) to remove any further impurities and inspected for any other impurities as precipitation. The final biodiesel yield quantity was weighted after completing all the purification processes. Biodiesel fuels are often kept in coloured, airtight containers with correct labelling and standard hazard codes in accordance with the biodiesel handling policy guide to preserve the fuel from

photo-oxidation (Alleman et al., 2016). Equation (1) was used to obtain the fuel conversion or FAME yield efficiency (%Y):

$$\%Y = \frac{\text{Weight of biodiesel fuel}}{\text{Weight of the oil}} \times 100 \quad (1)$$

## 2.2.2 Transesterification process optimisation

The acid value of the canola oil was found to be 1.453 (0.73% FFA content). A three-factor-three-level Box–Behnken (BB) was employed in the modelling and optimisation studies, which generated 15 experimental runs that were subsequently carried out. The independent variables considered for the optimisation include methanol–oil ratio, catalyst amount, and reaction temperature. The coded and uncoded levels of the independent variables are shown in Table 1. The process yield was modelled using a quadratic model, as illustrated in Eq. (2).

$$Y = a_0 + a_1x_1 + a_2x_2 + a_3x_3 + a_{11}x_1^2 + a_{22}x_2^2 + a_{33}x_3^2 + a_{12}x_{12} + a_{13}x_{13} + a_{23}x_{23} \quad (2)$$

Here,  $Y$  is the yield of the analysis, known as the predicted value. The subordinate values 1, 2, 3 indicate the three individual parameters in the model, 'x' is the variable parameter, and 'a' is the corresponding term's coefficient.

Based on the algorithm, 15 small scale transesterification processes were carried out to obtain the experimental yield results, which were later imported to Minitab 18.0 for RSM analysis. RSM was performed as per the BB model to conduct the canola oil's transesterification reaction's statistical optimisation process. The experimental design as follows: 5:1 M, 6:1 M, 7:1 M (methanol to oil), 0.5%, 1%, 1.5% (wt%/wt. of oil) KOH and 50 °C, 55 °C, 60 °C reaction temperatures. The stirring speed of the reactor was maintained at 600 rpm for 120 min with a magnetic stirrer. Analysis of variances (ANOVA) was also performed for the data set to determine the statistical significance of the experimental data and the predicted data.

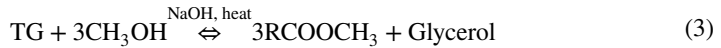
## 2.2.3 Kinetic modelling of transesterification reaction

It is critical to understand the reaction mechanism of the transesterification process to determine the kinetics of the chemical processes. As per the stoichiometry of the transesterification process, one mole (1 M) of fat or oil (triglycerides, TG) react with three moles (3 M) of  $\text{CH}_3\text{OH}$  in the presence of alkali catalysts (e.g., NaOH or KOH) to produce 3 mol (3 M) of FAME ( $\text{RCOOCH}_3$ ) and glycerol. This is a reversible chemical reaction. Therefore, sufficient methanol is utilised in practice to reduce process efficiency loss owing to reverse reaction.

**Table 1** Box-Behnken Design summary for transesterification process of canola oil

Operation parameters	Unit	Symbol	Range and coded levels		
			−1	0	+1
Methanol: oil	M/M	$M$	5	6	7
Alkali catalyst (KOH)	wt.%	$B$	0.5	1.0	1.5
Temperature	°C	$T$	50	55	60

The transesterification process is a combination of three steps of reaction mechanisms. Along with the degraded glyceride, a certain quantity of FAME is created in each phase. In the first stage, the triglycerides (TG) are transformed into diglycerides (DG) by interacting with a stoichiometric amount of 1 M CH<sub>3</sub>OH. Another mole of CH<sub>3</sub>OH is used to convert the DG into monoglycerides (MG) alongside the FAME generated in the second step. In the third step, another mole of CH<sub>3</sub>OH is used to convert the MG into glycerol (G) and FAME. As shown in Eq. 3, the complete process (i.e., stoichiometric) may be theoretically simplified as a shunt reaction.



Because of the large quantity of methanol consumed in the transesterification process in the actual instance, the reaction rate is a pseudo-forward reaction. Andreo-Martínez et al. (2018) mentioned that the transesterification rate reaction could be either of the pseudo-zero order, pseudo-first-order and pseudo-second-order reaction process. In that case, an apparent reaction rate constant ( $k_1$ ) can be determined to express the conversion rate of TG into FAME. Kusdiana and Saka (2001) mentioned that the mixture is a combination of converted methyl esters (ME) and unmethyl ester (uME) during the transesterification process within a batch reactor, and the reaction rate can be described as a pseudo-first-order reaction. Based on the analyses given for pseudo-first-order irreversible reaction rate (Andreo-Martínez et al., 2018; Kusdiana & Saka, 2001) characteristics of transesterification reaction, the kinetics of conversion of TG into FAME can be presented as in Eq. (4).

$$\ln(1-x) = -k_1t, \text{ or } -\ln(1-x) = k_1t \quad (4)$$

Here,  $x$  is considered as a fractional conversion entity of FAME in the batch reactor, and  $k_1$  is the apparent reaction rate constant.

Based on the experimental results, a graphical plot can be depicted between " $-\ln(1-x)$ " and " $t$ " to determine the value of reaction rate constant  $k_1$  at given operating conditions.

Therefore, in the following derivation of Andreo-Martínez et al. (2018), the overall reaction rate (kinetic model of the transesterification process) can be expressed as in Eq. (5).

$$r = -\frac{dC_{\text{TG}}}{dt} = k_1 C_{\text{TG}} = Ae^{\left[-\frac{E_a}{RT}\right]} C_{\text{TG}} \quad (5)$$

Here,  $r$  is the reaction rate for the shunt reaction of the transesterification process,  $C_{\text{TG}}$  is the molar concentration of triglycerides,  $k_1$  is the overall apparent reaction rate constant and  $\left(-\frac{dC_{\text{TG}}}{dt}\right)$  is the rate of decay of TG with respect to time to produce the respective FAME.

Equation (5) can also be compared with the Arrhenius equation in Eq. (6):

$$k_1 = Ae^{\left[-\frac{E_a}{RT}\right]} \quad (6)$$

Here,  $k_1$  = reaction rate constant,  $A$  = frequency parameter of the reaction,  $R$  = universal gas constant ( $8.314 \text{ J mol}^{-1} \text{ K}^{-1}$ ),  $E_a$  = activation energy (kJ/mol) of the reaction process, and  $T$  = reaction temperature in Kelvin scale.

The logarithm form of the Arrhenius equation can be expressed as in Eq. (7).

$$\ln k_1 = \ln A + \left(-\frac{E_a}{R}\right) \frac{1}{T} \quad (7)$$

Equation (7) indicates that when different  $k_1$  values (as obtained by Eq. 4) are plotted against different  $T$  values, a straight line can be obtained for the " $\ln k_1$  versus  $1/T$ " relation. As a result, the values of  $A$  and  $E_a$  are determined, respectively, as the intercept and slope of the line for the considered reaction process.

On the other hand, when the transesterification process is considered only as a pseudo-homogenous irreversible process without a prior assumption of reaction order, Eq. (8) can be presented as demonstrated by Cheng et al. (2008).

$$\ln \left( \frac{dx}{dt} \right) = \ln k' + n \ln [C_{TG}(1-x)] \quad (8)$$

Here,  $x$  is considered as a fractional conversion entity of FAME in the batch reactor,  $\left( \frac{dx}{dt} \right)$  is the rate of production of FAME,  $n$  is the reaction order.

The relation of reaction rate constant  $k'$  in Eq. (8) to the overall reaction rate constant of the forward reaction ( $k_1$ ) is shown in Eq. (9):

$$k' = k_1 / C_{TG} \text{ or } k_1 = k' \times C_{TG} \quad (9)$$

The pseudo-homogenous irreversible transesterification reaction rate follows the relationship as presented in Eq. (10).

$$r = k C_{TG}^n = A e^{\left[ -\frac{E_a}{RT} \right]} [C_{TG}^n] \quad (10)$$

In this study, both reaction rate Eqs. (4) and (8) were investigated to determine the kinetic model of canola oil's transesterification reaction.

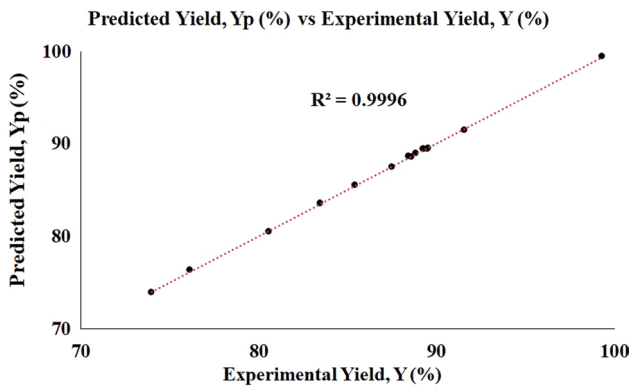
## 3 Results

### 3.1 Canola oil transesterification optimisation

The required experimental data for yield efficiency ( $Y$ ) of CB conversion for these parameters were acquired based on the designed parameter sets provided in Table 2. All of the intended transesterification processes of canola oil took 120 min to complete. The RSM analysis generated anticipated data for yield efficiency ( $Y_p$ ) based on the quadratic model for regression analysis (Eq. 2), as shown in Table 2. The highest yield was observed as 99.32% (experimental) and 99.45% (predicted) for the experimental conditions of 6 M methanol, 0.5% KOH catalyst with respect to oil weight, and reaction temperature of 60 °C. The minimum yield was 73.98% (experimental) and 73.92% (predicted) for the experimental conditions of 5 M, 1% KOH, and 50 °C. Figure 1 shows the regression fit between the experimental and predicted yield results of the RSM study for biodiesel synthesis from canola oil.

**Table 2** RSM analysis of transesterification process of canola oil

Run order	<i>M</i>	<i>B</i>	<i>T</i>	Experimental yield, <i>Y</i> (%)	Predicted yield, <i>Y<sub>p</sub></i> (%)
3	5	1	60	87.53	87.46
4	5	1.5	55	76.14	76.32
7	5	0.5	55	89.55	89.48
15	5	1	50	73.98	73.92
1	6	1.5	50	80.59	80.46
2	6	0.5	60	99.32	99.45
8	6	1.5	60	88.62	88.51
10	6	1	55	89.25	89.36
11	6	0.5	50	88.47	88.59
12	6	1	55	89.31	89.36
13	6	1	55	89.52	89.36
5	7	1	50	83.47	83.54
6	7	1.5	55	85.42	85.49
9	7	1	60	88.87	88.92
14	7	0.5	55	91.58	91.39

**Fig. 1** Regression fit between the predicted and experimental yield of canola biodiesel

### 3.1.1 Response surface regression

The regression analysis was conducted to a full quadratic model (Eq. 2) to predict the yield of CB. As per the analysis, the full regression Equation (uncoded) was derived as presented in Eq. (11). In Sect. 3.1.4, a quick description of the standardised effects of process parameters is offered using both the normal plot (Fig. 2) and the Pareto chart (Fig. 3).

$$\begin{aligned} \text{Yield, } Y_p(\%) = & 89.36 + 2.7675M - 4.7687B + 4.7288T - 4.7375M^2 + 1.05B^2 \\ & - 1.16T^2 + 1.8125MB - 2.0375MT - 0.705BT \end{aligned} \quad (11)$$



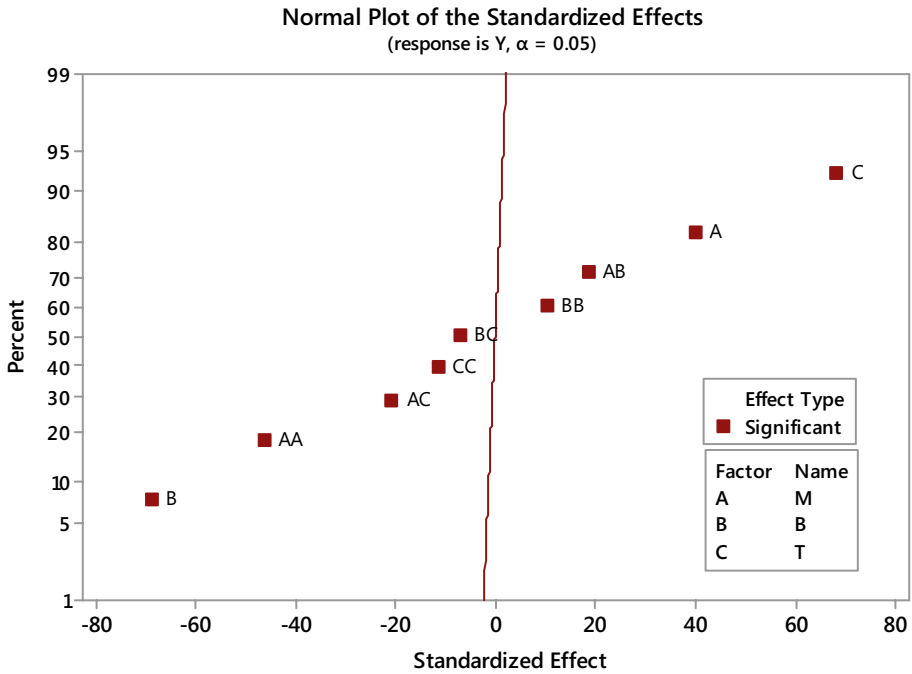


Fig. 2 Normal plot of the standardised effects in the transesterification process

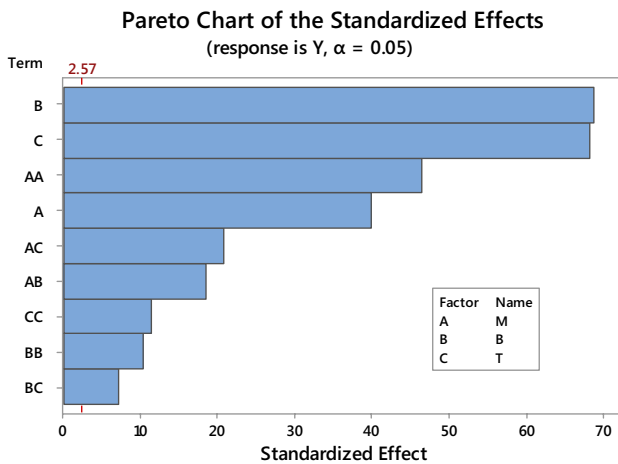


Fig. 3 Pareto chart for standardised effects in the transesterification process

### 3.1.2 Response optimisation

The limiting values of the factors and the regression fit for the optimisation are shown in Table 3. It shows that the optimal yield could be about 99.5% with the reaction conditions 5.89 M: 1 M methanol to oil molar ratio, 0.5% (w/w) KOH, at 60 °C reaction

**Table 3** Optimal response for the transesterification process of CB by RSM analysis

Variables	<i>M</i>	<i>B</i>	<i>T</i>	<i>D</i>
Optimal values	6.77	0.995	60	120
Response	Fit	SE Fit	95% CI	95% PI
Acidity removed	98.7	0.086	(99.1, 99.9)	(98.9, 100)

temperature and 120 min of reaction period in a batch reactor system. The 95% confidence interval also lies between 98.5 and 98.9, a narrow range of standard distribution for highly acceptable data analysis.

### 3.1.3 Analysis of variance (ANOVA) for transesterification process of canola oil

The analysis of variance (ANOVA) has been performed (Table 4) for the multivariable data set presented in Table 3, along with RSM analysis, to determine the statistical significance of the variables. Table 4 shows that the *P* values are less than 0.05 for all except the lack-of-fit error term. The difference of *F* value for the model with respect to the *F* value for the lack-of-fit is so high that the term does not bother the model's significance with these data. The standard deviation ( $S=0.196$ ) is a very good range of distributing 95% of the considered data, which results in a high value of *R* squared

**Table 4** ANOVA test of canola oil transesterification process yield prediction (coded parameters)

Source	DF	Seq SS	Contribution (%)	Adj SS	Adj MS	<i>F</i> value	<i>P</i> value
Model	9	547.13	99.96	547.13	60.79	1582.09	0
Linear	3	422.09	77.12	422.09	140.69	3661.58	0
<i>M</i>	1	61.27	11.20	61.27	61.27	1594.60	0
<i>B</i>	1	181.92	33.24	181.92	181.92	4734.62	0
<i>T</i>	1	178.89	32.68	178.89	178.89	4655.53	0
Square	3	93.30	17.05	93.30	31.10	809.38	0
<i>M</i> * <i>M</i>	1	83.51	15.26	82.87	82.87	2156.66	0
<i>B</i> * <i>B</i>	1	4.82	0.88	4.07	4.071	105.94	0
<i>T</i> * <i>T</i>	1	4.96	0.91	4.96	4.96	129.3	0
Two-way interaction	3	31.73	5.80	31.73	10.57	275.29	0
<i>M</i> * <i>B</i>	1	13.14	2.40	13.14	13.14	341.98	0
<i>M</i> * <i>T</i>	1	16.60	3.03	16.60	16.66	432.16	0
<i>B</i> * <i>T</i>	1	1.98	0.36	1.98	1.98	51.74	0.001
Error	5	0.19	0.04	0.19	0.03		
Lack-of-Fit	3	0.15	0.03	0.15	0.05	2.52	0.297
Pure error	2	0.04	0.01	0.04	0.02		
Total	14	547.32	100.00				
<i>S</i>		<i>R</i> -sq	<i>R</i> -sq (adj)		PRESS		<i>R</i> -sq (pred.)
Model summary							
0.196		99.96%	99.90%		2.52		99.54%

**Table 5** Coefficients of the regression fit and VIF values for transesterification process of canola oil (coded parameters)

Term	Coefficients	SE coefficients	95% CI	T value	P value	VIF
Constant	89.36	0.11	(89.07, 89.65)	789.58	0	
<i>M</i>	2.78	0.07	(2.59, 2.95)	39.93	0	1
<i>B</i>	-4.77	0.07	(-4.95, -4.59)	-68.81	0	1
<i>T</i>	4.72	0.07	(4.55, 4.91)	68.23	0	1
<i>M*M</i>	-4.74	0.10	(-5.00, -4.48)	-46.44	0	1.01
<i>B*B</i>	1.05	0.10	(0.78, 1.31)	10.29	0	1.01
<i>T*T</i>	-1.16	0.10	(-1.42, -0.90)	-11.37	0	1.01
<i>M*B</i>	1.81	0.09	(1.56, 2.06)	18.49	0	1
<i>M*T</i>	-2.04	0.09	(-2.29, -1.79)	-20.79	0	1
<i>B*T</i>	-0.71	0.09	(-0.96, -0.45)	-7.19	0.001	1

value of 99.96%, *R* squared(adj) value of 99.90% and *R* squared(predicted) value of 99.54%.

On the other hand, from Table 5, the coefficient table from the RSM shows that the values of variables of inflation factors (VIF) are within the suitability region. The highest value of VIF was 1.01, whereas the acceptability level is under 5, i.e.  $VIF < 5$ . That means no multicollinearity effect creates any adverse effect on the parameters while building up the regression model coefficients.

### 3.1.4 Effect plots parameters for RSM analysis of canola oil transesterification process

Figure 2 (normal plot) and Fig. 3 (Pareto chart) are the graphical presentations of how the parameters of the quadratic regression model have influenced the transesterification process of canola oil.

The effectiveness ratio of all these parameters can be realised from either the Pareto chart or normal plot. It is only the normal plot that shows whether the significant terms are positively or negatively influencing the model prediction. The left-hand side of the t-statistics fit line is quantitative measures of significantly negative effect developing parameters. If the values of these parameters are increased from lower values towards higher values, the negative effect is reduced.

The normal plot in Fig. 2 shows the positive and negative effects of the significance of the quadratic model parameters while developing the predicted model of response. Figure 2 indicates that the higher amount of catalyst had a negative impact on the transesterification process yield of canola oil, whereas the reaction temperature has the most positive significant contribution towards the process yield. Any parameters that are insignificant are shown on the line of the t-distribution standardisation line on the normal plot. There are two insignificant terms in the model response, which are coded as BD and AD, i.e., mutual interactions of "catalyst content \* reaction time" and "methanol content \* reaction time".

The Pareto chart (Fig. 3), on the other hand, only indicates which parameters are significantly effective and insignificant in the predicted models. The Pareto chart shows a threshold value of significance level. If the standardised effects of the parameters are lower than the threshold values, the effect is insignificant. Figure 3 shows that the significance level is 2.57 for the terms, and none of the terms was below that level. So, all the parameters

considered in the analysis process models were significantly affecting the reaction output (either in the positive or negative way, as presented in the normal plot).

### 3.1.5 Response surface plots to show the relative effects of parameters on %yield of canola oil transesterification process

Both the 2D contour plot and the 3D response surface plot are presented to show the effects of two independent variables on the %yield of CB obtained from the transesterification processes. When the effect of two variables was observed, the other variable was kept constant at its respective optimal value within the process. Also, the reaction period was kept constant at 120 min always. Figures 4, 5 and 6 show a total of three combinations of two variables from three independent parameters: namely, methanol to esterified canola oil molar ratio ( $M$ ), amount of KOH catalyst ( $B$ ), and reaction temperature ( $T$ ) and their effects are discussed in the following sections.

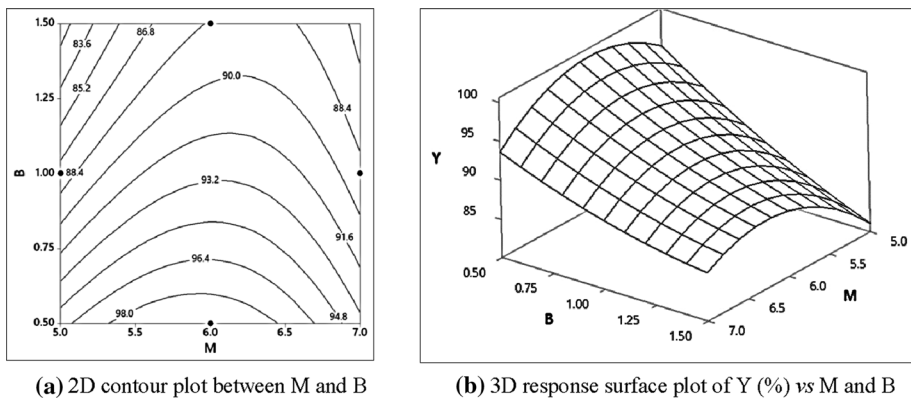


**Fig. 4** Interaction effects of methanol to oil molar ratio ( $M$ ) and KOH catalyst content ( $B$ ) on canola FAME yield ( $Y$ )

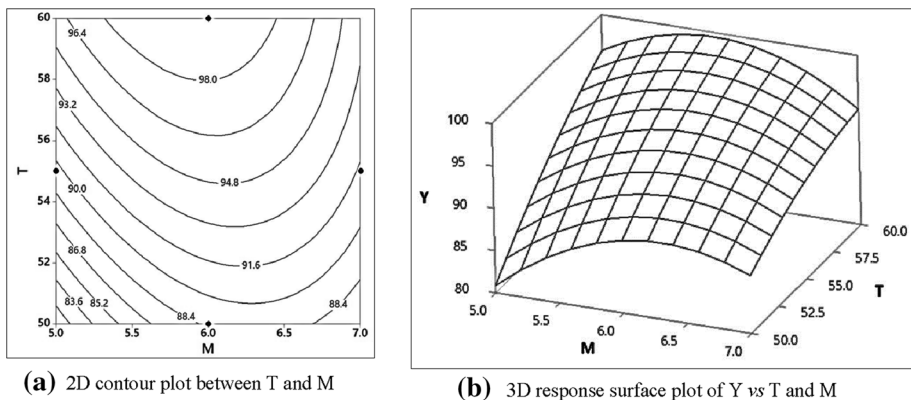


**Fig. 5** Interaction effects of reaction temperature ( $T$ ) and methanol to oil molar ratio ( $M$ ) on canola oil FAME yield ( $Y$ )

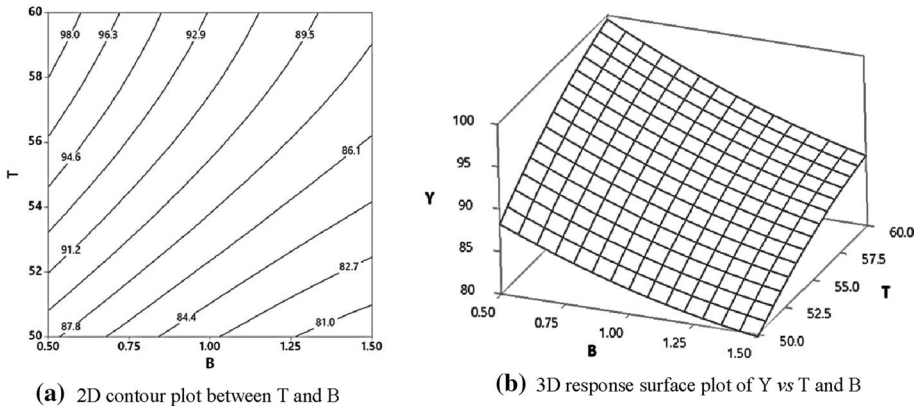


**Fig. 6** Interaction effect of reaction temperature ( $T$ ) and catalyst content ( $B$ ) on FAME yield ( $Y$ ) of the transesterification process canola oil

**3.1.5.1 Effects of catalyst content ( $B$ ) and methanol to oil ratio ( $M$ )** Figure 4a and b shows that the range of methanol content varied from 5 to 7 M, whereas the catalyst content varied from 0.5 to 1.5 wt% of the refined canola oil. The surface diagram shows that the peak yield of the transesterification process lies at the intersection between 0.5% catalyst and about 6 M methanol content. The contour plot shows that higher yield contour lines need a lesser catalyst and the range of methanol required to obtain the desired yield. It can be seen from the contours plot that 98% yield could be obtained for the methanol range of 5.35–6.45 M and catalyst range of 0.5–0.6% while the temperature was kept constant at 60 °C.

**3.1.5.2 Effect of methanol to oil ratio ( $M$ ) and reaction temperature ( $T$ )** Figure 5a and b shows the response of transesterification based on the variation of  $T$  and  $M$ , while the other parameter  $B$  was kept constant at the optimal level. The contour graph shows that the higher the temperature, the higher is the yield contour line for any methanol content. However, beyond 95% yield, the methanol range shrinks for the temperature range of the reaction. The 3D surface diagram shows the yield increment with the increase in  $M$  for constant temperature until it reaches a peak point near 6 M of methanol content. After this point addition of methanol reduces the yield quantity. Again, at any constant methanol content, the increase in temperature has a higher impact on increasing the yield. While combining the effects of  $T$  and  $M$ , the peak surface point can be observed at the intersection of 60 °C and about 6 M methanol line.

**3.1.5.3 Effects of methanol to reaction temperature ( $T$ ) and catalyst content ( $B$ )** Figure 6a and b shows that the increased amount of  $T$  and a reduction of  $B$  had a positive effect on the biodiesel yield of canola oil. The contour lines are diagonally distributed on the  $T$  versus  $B$  graph. As a result, the surface responses show a decrease in yield with the increase of catalyst content at any temperature. Thus, the temperature effect has positive significance in increasing the yield at any catalyst considered within the range. The surface has a peak around the very corner of the intersection between 0.5% catalyst and 60 °C temperature lines. Indeed, this condition is achieved when the reaction duration is 120 min, and methanol content is kept constant at its optimal value. This response curve also indicates the optimal ranges of the model.

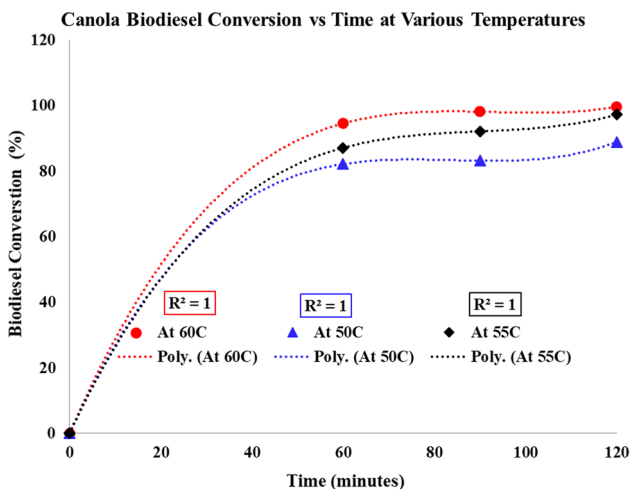


Fig. 7 Canola oil biodiesel (CB) conversion at various times at 60 °C, 55 °C and 50 °C

### 3.2 Determination of kinetic model for transesterification process of canola oil

Based on the optimisation process analysis, the maximum predicted yield of biodiesel could be obtained for 5.9 M: 1 M methanol to canola oil molar ratio, 0.5% (w/w) KOH catalyst with respect to the canola oil quantity, reaction temperature 60 °C and the reaction duration of 120 min. In order to determine the chemical kinetics of the transesterification process of canola oil, both the methanol to oil ratio and the catalyst contents were kept constant. The other two parameters, i.e., reaction temperature and the reaction duration, were varied from 50–60 °C and 0–120 min, respectively. The transesterification reactions were observed at various times for each of the temperatures considered in this study. Overall, three sets of transesterification reactions were observed. Figure 7 shows the polynomial regression fit of the experimentally obtained biodiesel conversion at various times at 60 °C, 55 °C and 50 °C. The  $R$  square values in the polynomial regression fit show very good conformity of the achieved results for the polynomial regression fits.

#### 3.2.1 Reaction kinetic model for pseudo-first-order transesterification process

Here, the kinetic model was determined by following the kinetic mechanism of the transesterification process described in Sect. 2.2.3. When  $x$  is considered as a fractional conversion entity of methyl ester from canola oil in the batch reactor, Eq. (4) can be used to determine the reaction kinetics for a pseudo-first-order homogenous irreversible transesterification reaction. Hence, for various values of  $T$ , the plot between  $-\ln(1-x)$  and  $t^n$  can be plotted in Fig. 8. It can be observed that the  $R$ -square values are a good fit.

By comparing the regression fits of Fig. 9 with Eq. (4), the values of  $k_1$ ,  $1/T$  and  $\ln k_1$  could be obtained as presented in Table 8. Also, the values of  $1/T$  and  $\ln k_1$  from Table 6 can be plotted to obtain a line with slope and interception, as shown in Fig. 9, to determine the activation energy ( $E_a$ ) as the slope of the curve.

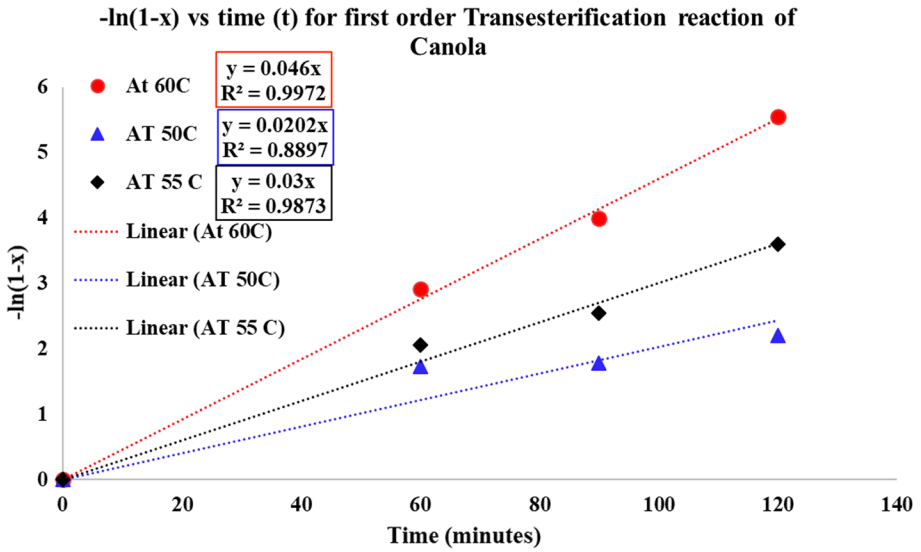


Fig. 8 Determination of reaction rate constant for the transesterification process of canola oil

Fig. 9. 1/T versus lnk<sub>1</sub> plot to determine activation energy (E<sub>a</sub>) and frequency factor (A<sub>p</sub>) for the transesterification process of canola oil

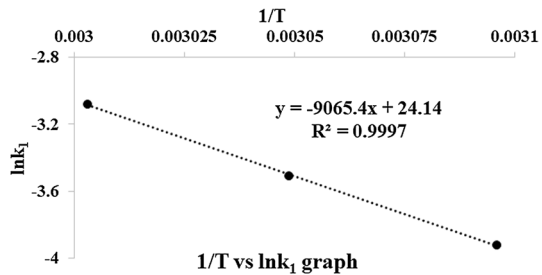


Table 6 Determination of 1/T and lnk<sub>1</sub> for canola oil transesterification kinetics

T (°C)	T (k)	Rate constant, k <sub>1</sub> (1/mol.min)	R-sq value	1/T	lnk <sub>1</sub>
60	333	0.046	0.993	0.003003	-3.0791139
55	328	0.03	0.9593	0.003049	-3.5065579
50	323	0.0198	0.932	0.003096	-3.9220733

The derived activation energy and frequency factors determined by comparing the regression Equation of Fig. 9 with the logarithmic form of the Arrhenius equation (Eq. 7) were 75.36974 kJ/mol and  $3.05 \times 10^{10} \text{ min}^{-1}$ , respectively. Therefore, the values obtained could be put in Eq. (5) to obtain the reaction kinetic model (Eq. 12) for a pseudo-first-order homogenous irreversible transesterification reaction following Eq. 5a, the overall reaction rate (kinetic model of transesterification process) can be expressed as follows:

$$r = -\frac{dC_{TG}}{dt} = k_1 C_{TG} = A e^{\left[-\frac{E_a}{RT}\right]} C_{TG} = 3.05 \times 10^{10} e^{\left[-\frac{75.37}{RT}\right]} C_{TG} \tag{12}$$

Kumar and Kiriamiti (2020) reported an activation energy of 71.3 kJ/mol for homogeneous NaOH based transesterification of *Croton megalocarpus* oil.

### 3.2.2 Reaction kinetic model for pseudo-homogenous irreversible transesterification process

As mentioned in Sect. 2.2.3, if the reaction order is not assumed earlier, the kinetic model can be developed by assuming pseudo-homogenous irreversible transesterification process (Eq. 8) (Cheng et al., 2008). Here, the vertical line presents data for  $\ln\left(\frac{dx}{dt}\right)$  and the horizontal line represents data for  $\ln[C_{TG}(1-x)]$  when comparing with Eq. (8). The regression fits in Fig. 10 show a very good R-square fit. The slopes of these regression Equations from the curve fits present the respective reaction orders of the process.

While comparing the regression fits of Fig. 11 with Eq. (8), the average reaction order and the reaction rate constants can be determined as in Table 7. Therefore, values of  $1/T$  and  $\ln k$  from Table 7 can be used to produce the graph between " $1/T$  and  $\ln k$ " as presented in Fig. 10. The slope of the graph can be used to determine the activation energy of the process kinetics.

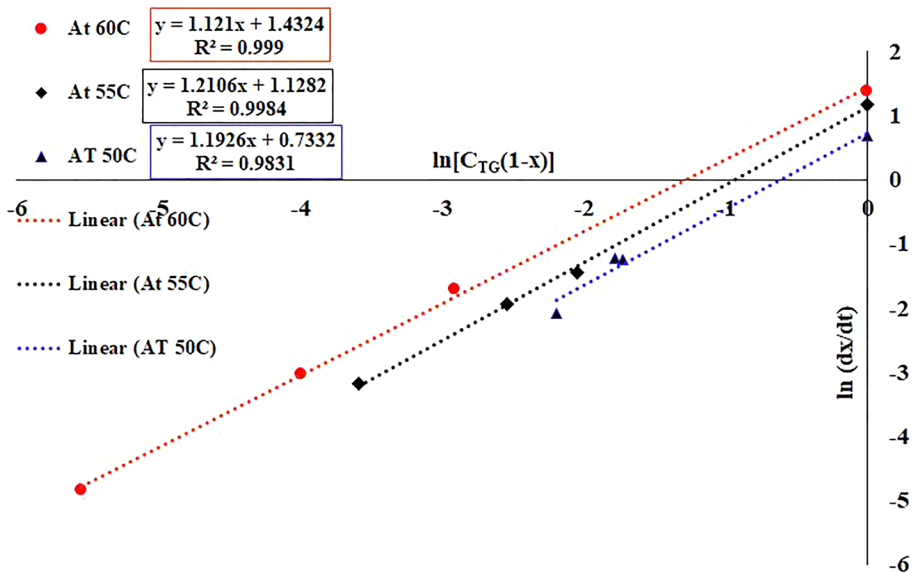


Fig. 10  $\ln(dx/dt)$  versus  $\ln C_{TG}(1-x)$  graph plot for reaction kinetics of canola oil transesterification in case of a pseudo-homogenous irreversible reaction



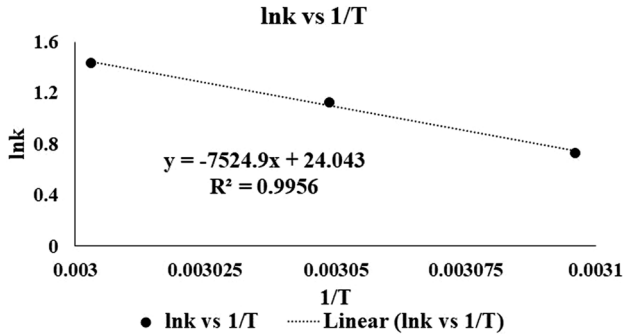


Fig. 11 1/T versus lnk graph for activation energy determination of canola oil transesterification process

Table 7 1/T versus lnk graph for canola oil transesterification process kinetics

T (°C)	T (K)	n (order)	Lnk'	k'	k = k' × C <sub>TG</sub>	1/T	lnk	Average reaction order, n
60	333	1.1218	1.4324	4.1887401	4.18874	0.003003	1.4324	1.175
55	328	1.2106	1.1282	3.0900893	3.090089	0.003049	1.1282	
50	323	1.1926	0.7332	2.0817315	2.081732	0.003096	0.7332	

By comparing the regression fit of Fig. 11 with the Arrhenius Equation logarithmic form (Eq. 7), the activation energy and frequency factors were calculated to be 62.577068 kJ/mol and  $2.77 \times 10^{10} \text{ min}^{-1}$ , respectively. When the process is considered a pseudo-homogenous irreversible reaction process, the values may be utilised in Eq. (10) to create the reaction kinetic model for the transesterification of canola oil. The developed kinetic model is presented in Eq. (13). The reaction order is 1.18, activation energy is 62.58 kJ/mol, and the frequency factor is  $2.77 \times 10^{10} \text{ min}^{-1}$ .

$$r = kC_{TG}^n = Ae^{\left[-\frac{E_a}{RT}\right]} [C_{TG}^n] = 2.77 \times 10^{10} e^{\left[-\frac{62.58}{RT}\right]} C_{TG}^{1.18} \tag{13}$$

### 3.3 Fuel composition

The fatty acid composition of the produced biodiesel through the optimisation process is shown in Table 8. From the table, it can be seen that Australian canola oil is mostly composed of methyl ricinoleate, with 88.53 wt% included in the composition. This is followed by 5.58 wt% and 3.85 wt% methyl linoleate and methyl oleate, respectively. A clear difference is observed compared to the FAC reported by Issariyakul and Dalai (2010). The main component of their canola oil biodiesel is methyl oleate which contains 60.92 wt% of this component. Based on the composition, canola biodiesel contains a total of 1.58 wt% saturated FAME component, 92.38 wt% monounsaturated FAME and 6.04 wt% polyunsaturated FAME. Table 9 compares the properties of produced canola biodiesel and diesel. According to the table, canola oil biodiesel has a 21.5% higher cetane number but a 6% lower LHV than diesel fuel.

**Table 8** Fatty acid composition of the produced canola biodiesel

FAME group	Linear structure	Canola biodiesel (wt. %)	Canola oil (wt. %) (Issariyakul & Dalai, 2010)
C16:0	$\text{CH}_3(\text{CH}_2)_{14}\text{COOCH}_3$ (Methyl palmitate)	0.72	4.36
C16:1	$\text{CH}_3(\text{CH}_2)_5\text{CH}=\text{CH}(\text{CH}_2)_7\text{COOCH}_3$ (Methyl palmitoleate)	–	0.16
C17:0	$\text{CH}_3(\text{CH}_2)_{15}\text{COOCH}_3$ (Methyl heptadecanoate)	–	–
C18:0	$\text{CH}_3(\text{CH}_2)_{16}\text{COOCH}_3$ (Methyl stearate)	0.55	1.96
C18:1	$\text{CH}_3(\text{CH}_2)_7\text{CH}=\text{CH}(\text{CH}_2)_7\text{COOCH}_3$ (Methyl oleate)	3.85	60.92
C18:1(OH)	$\text{CH}_3(\text{CH}_2)_5\text{CH}(\text{OH})\text{CH}_2\text{CH}=\text{CH}(\text{CH}_2)_7\text{COOCH}_3$ (Methyl ricinoleate)	88.53	2.89
C18:2	$\text{CH}_3(\text{CH}_2)_4\text{CH}=\text{CHCH}_2\text{CH}=\text{CH}(\text{CH}_2)_7\text{COOCH}_3$ (Methyl linoleate)	5.58	18.70
C18:3	$\text{CH}_3\text{CH}_2\text{CH}=\text{CHCH}_2\text{CH}=\text{CH}(\text{CH}_2)_7\text{COOCH}_3$ (Methyl linolenate)	0.46	6.79
C20:0	$\text{CH}_3(\text{CH}_2)_{18}\text{COOCH}_3$ (Methyl arachidate/Arachidic acid)	0.31	0.59

**Table 9** Comparison of physicochemical properties of canola biodiesel and diesel

Physicochemical properties	Canola biodiesel	Diesel
Kinematic viscosity (mm <sup>2</sup> /s, at 40 °C)	4.56	3.34
Density (g/cm <sup>3</sup> , at 15 °C)	0.883	0.833
Higher heating value (MJ/kg, HHV)	40.99	45.67
Lower heating value (MJ/kg, LHV)	39.61	42.30
Oxidation stability (hours, at 110 °C)	10.42	39.50
Flash point (°C)	170.2	69.00
Pour point (°C)	−8	0.00
Cloud point (°C)	−1.8	8.00
Cold filter plugging point (°C, CFPP)	−7.9	5.00
Cetane number (CN)	58.32	48.00
Iodine value (IV, g I <sub>2</sub> /100 g oil)	126.1	NA
Saponification value (SV, mg KOH/ g oil)	201.15	NA
Acid value (AV, mg KOH/g oil)	1.45	0.06

## 4 Discussion

Table 10 summarises the transesterification process parameters (optimal) and kinetic parameters such as activation energy ( $E_a$ ), frequency factor ( $A$ ), reaction rate constant ( $k$ ), and canola oil reaction model based on various research studies. It has been observed that there is a scarcity of transesterification process optimisation and reaction kinetic modelling for the typical batch process with homogeneous alkaline catalysts. Table 10 shows that the methanol-to-oil ratio fluctuates significantly, and the catalyst utilised was both homogeneous and heterogeneous. In general, activation energy ( $E_a$ ) is the smallest amount of energy held by colliding molecules towards the formation of the product (Mercy Nisha Pauline et al., 2021). In general, a steeper Arrhenius plot indicated greater activation energy of the transesterification process, while a flat slope suggested a low  $E_a$ . A higher  $E_a$  value indicates a slower reaction rate, which may be countered by adding a catalyst or raising the reaction temperature. Furthermore, increasing the solvent concentration and utilising microwave or ultrasonication to facilitate transesterification may reduce this even further. Also, greater  $E_a$  responses fluctuate faster across the same temperature range and are more sensitive to temperature variations.

## 5 Conclusions

The study's main objectives were to investigate the optimal reaction parameters for the transesterification process in a conventional reactor and develop the kinetic reaction models for biodiesel production per the optimised process conditions from this oil feedstock. RSM analyses performed optimisation to determine the best possible parametric quantity within the considered range of operating parameters. The Box–Behnken algorithm was used to design the required number of experiments based on 3 factors and 3 levels matrix. A total of 15 reactions were performed according to this algorithm, and all the results were imported to the statistical software Minitab 18.0. In addition, multivariable ANOVA was performed to determine the effectiveness of parameters used in the regression

**Table 10** Optimal reaction parameters and kinetics of the transesterification process of oil

Feedstock	Methanol: Oil molar ratio	Catalyst (% w/v of oil)	Biodiesel yield (%)	Temperature (°C)	Time (minutes)	Kinetic parameters	References
Canola oil	12.3:1	9.03% KOH/ZSM-5-Fe <sub>3</sub> O <sub>4</sub>	93.6	65	196	Pseudo-first-order, Ea = 122.7 kJ, A = 2.15 × 10 <sup>17</sup> min <sup>-1</sup>	Rezayan and Taghizadeh (2018)
Canola oil	9:1	1% NaOH	90	65	7	Pseudo-first-order irreversible, K = 0.45	Zhou (2013)
Canola oil (Stepwise transesterification process in a membrane reactor)	24:1	0.5% NaOH	98	65	5	Homogenous reversible. Forward steps' rate constants 2.2, 22.4, 4.1. Reverse: 1.4, 35.7, 0.6 respectively (L/mol.min)	Cao et al. (2009)
Canola oil	16:1 ethanol: oil	2% Mg-Co-Al-La layered double hydroxide (LDH)	97	200	300	Pseudo-first-order irreversible, Ea = 60.5 kJ/mol	Li et al. (2009)
Canola oil	15:1	4% Nanomagnetic ZnO-BiFeO <sub>3</sub>	95.4	65	360	-	Salimi and Hosseini (2019)
Canola oil	15:1	1% Mesoporous sulfated Ti-SBA-15	91	200	240	-	Sharma et al. (2014)
Canola oil	15:1	5% Li-doped CaO-La <sub>2</sub> O <sub>3</sub>	96.3	65	150	-	Maleki et al. (2017)
Unrefined canola oil (multistage enzymatic process)	15.8% (w/w) methanol, 13.5% buffer solution	24.4% (1:1 mix of R. oryzae with C. rugosa)	88.9	45	3600	-	Jang et al. (2012)

**Table 10** (continued)

Feedstock	Methanol: Oil molar ratio	Catalyst (% w/v of oil)	Biodiesel yield (%)	Temperature (°C)	Time (minutes)	Kinetic parameters	References
Australian Canola oil	5.89:1	0.5% KOH	99.5	60	120	For pseudo-first-order homogeneous irreversible $E_a = 75,36974 \text{ kJ/mol}$ $A = 3.05 \times 10^{10} \text{ min}^{-1}$ For pseudo-homogeneous irreversible $E_a = 62,577068 \text{ kJ/mol}$ $A = 2.77 \times 10^{10} \text{ min}^{-1}$	This study

model. Once the optimisation was performed, and the mutual effects of these parameters to the respective process outputs were analysed, these optimised parameters were considered to influence respective process reaction kinetics (i.e., reaction rate constants, reaction order and activation energy, etc.). The optimal process conditions were obtained as methanol to canola oil molar ratio 5.89 M:1 M, KOH catalyst content 0.5 wt% of the canola oil, and reaction temperature of 60 °C for the constant reaction period of 120 min in a batch reactor system. With these conditions, the optimal yield was predicted as 99.5% with a 95% confidence interval ( $P < 0.991$ ,  $P < 0.999$ ). The experimental yield obtained was 99.6% as per the optimal conditions. Two different kinetic models were developed either by assuming reaction order or without assuming the reaction order. The activation energy and the frequency factors determined for kinetic models were 75.36974 kJ/mol and  $3.05 \times 10^{10} \text{ min}^{-1}$  (for pseudo-first-order homogenous irreversible) and 62.577068 kJ/mol and  $2.77 \times 10^{10} \text{ min}^{-1}$  (for pseudo-homogenous irreversible), respectively. This study has comprised an overall experimental and analytical procedure to investigate the biodiesel production processes from canola oil, one of the most popular feedstocks used in biodiesel production. The optimisation study and the kinetic determination can help determine the economic impact of advancing biodiesel production.

**Authors' contributions** MAH analysed, interpreted the data and wrote the article. IMRF and HCO modified and revised the article. MGR, MMKK, NA, and TMIM supervised the work and contributed to improving the manuscript. All authors read and approved the final manuscript.

**Funding** Open Access funding enabled and organized by CAUL and its Member Institutions. This work was supported by Universiti Tenaga Nasional grant no. IC6-BOLDREFRESH2025 (HCR) under the BOLD2025 Program and the research higher education division of CQUniversity, Queensland, Australia.

**Availability of data and materials** All data generated or analysed during this study are included in this published article.

**Code availability** Not applicable.

## Declarations

**Conflict of interest** The authors declare that they have no conflict of interest.

**Ethics approval and consent to participate** Not applicable.

**Consent for publication** Not applicable.

**Open Access** This article is licensed under a Creative Commons Attribution 4.0 International License, which permits use, sharing, adaptation, distribution and reproduction in any medium or format, as long as you give appropriate credit to the original author(s) and the source, provide a link to the Creative Commons licence, and indicate if changes were made. The images or other third party material in this article are included in the article's Creative Commons licence, unless indicated otherwise in a credit line to the material. If material is not included in the article's Creative Commons licence and your intended use is not permitted by statutory regulation or exceeds the permitted use, you will need to obtain permission directly from the copyright holder. To view a copy of this licence, visit <http://creativecommons.org/licenses/by/4.0/>.

## References

- AEGIC. (2017). *Australian Canola*. Australian Export Grains Innovation Centre. <https://www.aegic.org.au/australian-grains/canola/>.
- Agriculture and Horticulture Development Board (AHDB). (2020a). What is the difference between Canola and Rapeseed Oil? URL: <https://rapeseedoilbenefits.com/faqs/difference-canola-rapeseed-oil/>. *AHDB Cereals and Oilseeds*. <https://www.rapeseedoilbenefits.com/faqs/difference-canola-rapeseed-oil/>.
- AHDB. (2020b). Rapeseed oil benefits—What is the difference between Canola and Rapeseed Oil? *AHDB Cereals and Oilseeds*. <https://www.rapeseedoilbenefits.com/faqs/difference-canola-rapeseed-oil/>.
- Alleman, T. L., McCormick, R. L., Christensen, E. D., Fioroni, G., Moriarty, K., & Yanowitz, J. (2016). *Biodiesel handling and use guide*, 5th edn. [https://afdc.energy.gov/files/u/publication/biodiesel\\_handling\\_use\\_guide.pdf](https://afdc.energy.gov/files/u/publication/biodiesel_handling_use_guide.pdf).
- Ampah, J. D., Yusuf, A. A., Agyekum, E. B., Afrane, S., Jin, C., Liu, H., Fattah, I. M. R., Show, P. L., Shouran, M., Habil, M., & Kamel, S. (2022). Progress and recent trends in the application of nanoparticles as low carbon fuel additives—a state of the art review. *Nanomaterials*, *12*(9), 1515.
- Andreo-Martínez, P., García-Martínez, N., Durán-del-Amor, M. D. M., & Quesada-Medina, J. (2018). Advances on kinetics and thermodynamics of non-catalytic supercritical methanol transesterification of some vegetable oils to biodiesel. *Energy Conversion and Management*, *173*, 187–196. <https://doi.org/10.1016/j.enconman.2018.07.069>
- Atique, M. N., Imran, S., Razaq, L., Mujtaba, M. A., Nawaz, S., Kalam, M. A., Manzoore, E. M., Soudagar, A. H., Veza, I., & Arshad, A. (2022). Hydraulic characterization of Diesel, B50 and B100 using momentum flux. *Alexandria Engineering Journal*, *61*(6), 4371–4388. <https://doi.org/10.1016/j.aej.2021.09.064>
- Australian Export Grains Innovation Centre (AEGIC). (2017). *Australian Canola*. URL: <https://www.aegic.org.au/australian-grains/canola/>. Australian Export Grains Innovation Centre. <https://www.aegic.org.au/australian-grains/canola/>.
- Betiku, E., & Ajala, S. O. (2014). Modeling and optimization of *Thevetia peruviana* (yellow oleander) oil biodiesel synthesis via *Musa paradisiacal* (plantain) peels as heterogeneous base catalyst: A case of artificial neural network vs. response surface methodology. *Industrial Crops and Products*, *53*, 314–322. <https://doi.org/10.1016/j.indcrop.2013.12.046>
- Bohlouli, A., & Mahdavian, L. (2019). Catalysts used in biodiesel production: A review. *Biofuels*. <https://doi.org/10.1080/17597269.2018.1558836>
- Cao, P., Tremblay, A. Y., & Dubé, M. A. (2009). Kinetics of Canola oil transesterification in a membrane reactor. *Industrial and Engineering Chemistry Research*, *48*(5), 2533–2541. <https://doi.org/10.1021/ie8009796>
- Cheng, J., Li, Y., He, S., Shen, W., Liu, Y., & Song, Y. (2008). Reaction kinetics of transesterification between vegetable oil and methanol under supercritical conditions. *Energy Sources, Part a: Recovery, Utilization, and Environmental Effects*, *30*(8), 681–688. <https://doi.org/10.1080/15567030601082084>
- Choudhury, H. A., Srivastava, P., & Moholkar, V. S. (2014). Single-step ultrasonic synthesis of biodiesel from crude *Jatropha curcas* oil. *AIChE Journal*, *60*(5), 1572–1581. <https://doi.org/10.1002/aic.14371>
- Encinar, J. M., González, J. F., Martínez, G., & Nogales-Delgado, S. (2022). Transesterification of soybean oil through different homogeneous catalysts: Kinetic study. *Catalysts*, *12*(2), 146.
- Encinar, J. M., Pardo, A., Sánchez, N., & Nogales, S. (2018). Biodiesel by transesterification of rapeseed oil using ultrasound: A kinetic study of base-catalysed reactions. *Energies*, *11*(9), 2229.
- Fattah, I. M. R., Masjuki, H. H., Kalam, M. A., Hazrat, M. A., Masum, B. M., Imtenan, S., & Ashraf, A. M. (2014). Effect of antioxidants on oxidation stability of biodiesel derived from vegetable and animal based feedstocks. *Renewable and Sustainable Energy Reviews*, *30*, 356–370. <https://doi.org/10.1016/j.rser.2013.10.026>
- Fattah, I. M. R., Ong, H. C., Mahlia, T. M. I., Mofijur, M., Silitonga, A. S., Rahman, S. M. A., & Ahmad, A. (2020). State of the art of catalysts for biodiesel production. *Frontiers in Energy Research*. <https://doi.org/10.3389/fenrg.2020.00101>
- Fayyazi, E., Ghobadian, B., Najafi, G., Hosseinzadeh, B., Mamat, R., & Hosseinzadeh, J. (2015). An ultrasound-assisted system for the optimization of biodiesel production from chicken fat oil using a genetic algorithm and response surface methodology. *Ultrasonics Sonochemistry*, *26*, 312–320. <https://doi.org/10.1016/j.ultsonch.2015.03.007>
- Food and Agricultural Organization (FAO). (2019). Countries by commodity: Top 10 country production of rapeseed oil in 2018. *FAOSTAT*. [http://www.fao.org/faostat/en/#rankings/countries\\_by\\_commodity](http://www.fao.org/faostat/en/#rankings/countries_by_commodity).

- Gunstone, F. D., & Harwood, J. L. (2007). Occurrence and characterisation of oils and fats. In F. D. Gunstone, J. L. Harwood, & A. J. Dijkstra (Eds.), *The lipid handbook with CD-ROM* (3rd ed., pp. 37–142). CRC Press.
- Hoang, A. T., Ong, H. C., Fattah, I. M. R., Chong, C. T., Cheng, C. K., Sakthivel, R., & Ok, Y. S. (2021). Progress on the lignocellulosic biomass pyrolysis for biofuel production toward environmental sustainability. *Fuel Processing Technology*, 223, 106997. <https://doi.org/10.1016/j.fuproc.2021.106997>
- Imtenan, S., Varman, M., Masjuki, H. H., Kalam, M. A., Sajjad, H., Arbab, M. I., & Rizwanul Fattah, I. M. (2014). Impact of low temperature combustion attaining strategies on diesel engine emissions for diesel and biodiesels: A review. *Energy Conversion and Management*, 80, 329–356. <https://doi.org/10.1016/j.enconman.2014.01.020>
- Issariyakul, T., & Dalai, A. K. (2010). Biodiesel production from greenseed canola oil. *Energy and Fuels*, 24(9), 4652–4658. <https://doi.org/10.1021/ef901202b>
- Jang, M. G., Kim, D. K., Park, S. C., Lee, J. S., & Kim, S. W. (2012). Biodiesel production from crude canola oil by two-step enzymatic processes. *Renewable Energy*, 42, 99–104. <https://doi.org/10.1016/j.renene.2011.09.009>
- Kanca, A., & Temur, H. (2016). The effects of long-term storage on the cold flow properties and viscosity of canola-based biodiesel. *Energy Sources, Part a: Recovery, Utilization, and Environmental Effects*, 38(15), 2205–2210. <https://doi.org/10.1080/15567036.2015.1047066>
- Khan, H. M., Iqbal, T., Mujtaba, M. A., Soudagar, M. E. M., Veza, I., & Fattah, I. M. R. (2021). Microwave assisted biodiesel production using heterogeneous catalysts. *Energies*, 14(23), 8135.
- Knothe, G. (2005). Dependence of biodiesel fuel properties on the structure of fatty acid alkyl esters. *Fuel Processing Technology*, 86(10), 1059–1070. <https://doi.org/10.1016/j.fuproc.2004.11.002>
- Kumar, A., & Kiriamiti, H. K. (2020). Kinetics of transesterification of *Croton megalocarpus* oil using alkaline earth catalysts with conventional and microwave heating. *International Journal of Chemical Engineering*, 2020, 8841331. <https://doi.org/10.1155/2020/8841331>
- Kumar, S., Jain, S., & Kumar, H. (2017). Process parameter assessment of biodiesel production from a Jatropha–algae oil blend by response surface methodology and artificial neural network. *Energy Sources, Part a: Recovery, Utilization, and Environmental Effects*, 39(22), 2119–2125. <https://doi.org/10.1080/15567036.2017.1403514>
- Kusdiana, D., & Saka, S. (2001). Kinetics of transesterification in rapeseed oil to biodiesel fuel as treated in supercritical methanol. *Fuel*, 80(5), 693–698. [https://doi.org/10.1016/S0016-2361\(00\)00140-X](https://doi.org/10.1016/S0016-2361(00)00140-X)
- Li, E., Xu, Z. P., & Rudolph, V. (2009). MgCoAl–LDH derived heterogeneous catalysts for the ethanol transesterification of canola oil to biodiesel. *Applied Catalysis b: Environmental*, 88(1), 42–49. <https://doi.org/10.1016/j.apcatb.2008.09.022>
- Maleki, H., Kazemini, M., Larimi, A. S., & Khorasheh, F. (2017). Transesterification of canola oil and methanol by lithium impregnated CaO–La<sub>2</sub>O<sub>3</sub> mixed oxide for biodiesel synthesis. *Journal of Industrial and Engineering Chemistry*, 47, 399–404. <https://doi.org/10.1016/j.jiec.2016.12.011>
- Mercy Nisha Pauline, J., Sivaramakrishnan, R., Pugazhendhi, A., Anbarasan, T., & Achary, A. (2021). Transesterification kinetics of waste cooking oil and its diesel engine performance. *Fuel*, 285, 119108. <https://doi.org/10.1016/j.fuel.2020.119108>
- Milledge, J., Smith, B., Dyer, P., & Harvey, P. (2014). Macroalgae-derived biofuel: A review of methods of energy extraction from seaweed biomass. *Energies*, 7(11), 7194–7222. <https://doi.org/10.3390/en7117194>
- Mofijur, M., Masjuki, H. H., Kalam, M. A., Atabani, A. E., Rizwanul Fattah, I. M., & Mobarak, H. M. (2014). Comparative evaluation of performance and emission characteristics of *Moringa oleifera* and Palm oil based biodiesel in a diesel engine. *Industrial Crops and Products*, 53, 78–84. <https://doi.org/10.1016/j.indcrop.2013.12.011>
- Montgomery, D. C. (2013). *Design and analysis of experiments* (8th ed.). Wiley.
- Office of the Gene Technology Regulator (OGTR). (2018). *The biology of Brassica napus L. (Canola)*. URL: [http://www.ogtr.gov.au/internet/ogtr/publishing.nsf/content/canola-3/\\$FILE/biologycanola08\\_2.pdf](http://www.ogtr.gov.au/internet/ogtr/publishing.nsf/content/canola-3/$FILE/biologycanola08_2.pdf). A. Government. [http://www.ogtr.gov.au/internet/ogtr/publishing.nsf/content/canola-3/\\$FILE/biologycanola08\\_2.pdf](http://www.ogtr.gov.au/internet/ogtr/publishing.nsf/content/canola-3/$FILE/biologycanola08_2.pdf).
- Okwu, M. O., Samuel, O. D., Ewim, D. R. E., & Huan, Z. (2021). Estimation of biogas yields produced from combination of waste by implementing response surface methodology (RSM) and adaptive neuro-fuzzy inference system (ANFIS). *International Journal of Energy and Environmental Engineering*, 12(2), 353–363. <https://doi.org/10.1007/s40095-021-00381-5>
- Ong, H. C., Tiong, Y. W., Goh, B. H. H., Gan, Y. Y., Mofijur, M., Rizwanul Fattah, I. M., Chong, C. T., Alam, MAsrafu, Lee, H. V., Silitonga, A. S., & Mahlia, T. M. I. (2021). Recent advances in biodiesel production from agricultural products and microalgae using ionic liquids: Opportunities and



- challenges. *Energy Conversion and Management*, 228, 113647. <https://doi.org/10.1016/j.enconman.2020.113647>
- Ramos, M., Dias, P. A., Puna, F. J., Gomes, J., & Bordado, C. J. (2019). Biodiesel production processes and sustainable raw materials. *Energies*. <https://doi.org/10.3390/en12234408>
- Ranjitha, J., Gokul Raghavendra, S., Vijayalakshmi, S., & Deepanraj, B. (2020). Production, optimisation and engine characteristics of beef tallow biodiesel rendered from leather fleshing and slaughterhouse wastes. *Biomass Conversion and Biorefinery*, 10(3), 675–688. <https://doi.org/10.1007/s13399-019-00501-6>
- Rezayan, A., & Taghizadeh, M. (2018). Synthesis of magnetic mesoporous nanocrystalline KOH/ZSM-5-Fe<sub>3</sub>O<sub>4</sub> for biodiesel production: Process optimization and kinetics study. *Process Safety and Environmental Protection*, 117, 711–721. <https://doi.org/10.1016/j.psep.2018.06.020>
- Salimi, Z., & Hosseini, S. A. (2019). Study and optimization of conditions of biodiesel production from edible oils using ZnO/BiFeO<sub>3</sub> nano magnetic catalyst. *Fuel*, 239, 1204–1212. <https://doi.org/10.1016/j.fuel.2018.11.125>
- Samuel, O. D., & Okwu, M. O. (2019). Comparison of response surface methodology (RSM) and artificial neural network (ANN) in modelling of waste coconut oil ethyl esters production. *Energy Sources, Part a: Recovery, Utilization, and Environmental Effects*, 41(9), 1049–1061. <https://doi.org/10.1080/15567036.2018.1539138>
- Samuel, O. D., Okwu, M. O., Oyejide, O. J., Taghinezhad, E., Afzal, A., & Kaveh, M. (2020). Optimizing biodiesel production from abundant waste oils through empirical method and grey wolf optimizer. *Fuel*, 281, 118701. <https://doi.org/10.1016/j.fuel.2020.118701>
- Sharma, R. V., Baroi, C., & Dalai, A. K. (2014). Production of biodiesel from unrefined canola oil using mesoporous sulfated Ti-SBA-15 catalyst. *Catalysis Today*, 237, 3–12. <https://doi.org/10.1016/j.cattod.2014.07.005>
- Singh, D., Sharma, D., Soni, S. L., Sharma, S., Kumar Sharma, P., & Jhalani, A. (2020). A review on feedstocks, production processes, and yield for different generations of biodiesel. *Fuel*, 262, 116553. <https://doi.org/10.1016/j.fuel.2019.116553>
- Singh, T. S., Rajak, U., Samuel, O. D., Chaurasiya, P. K., Natarajan, K., Verma, T. N., & Nashine, P. (2021). Optimization of performance and emission parameters of direct injection diesel engine fuelled with microalgae *Spirulina* (L.)—Response surface methodology and full factorial method approach. *Fuel*, 285, 119103. <https://doi.org/10.1016/j.fuel.2020.119103>
- Su, G., Ong, H. C., Ibrahim, S., Fattah, I. M. R., Mofijur, M., & Chong, C. T. (2021). Valorisation of medical waste through pyrolysis for a cleaner environment: Progress and challenges. *Environmental Pollution*, 279, 116934. <https://doi.org/10.1016/j.envpol.2021.116934>
- UFOP. (2020a). *UFOP report on global market supply 2019/2020a*. [https://www.ufop.de/files/7515/7797/1943/WEB\\_UFOP\\_Global\\_Supply\\_Report\\_A5\\_EN\\_19\\_20.pdf](https://www.ufop.de/files/7515/7797/1943/WEB_UFOP_Global_Supply_Report_A5_EN_19_20.pdf).
- Union Zur Förderung Von Oel- Und Proteinpflanzen E.V. (UFOP). (2020b). *UFOP report on global market supply 2019/2020b*. [https://www.ufop.de/files/7515/7797/1943/WEB\\_UFOP\\_Global\\_Supply\\_Report\\_A5\\_EN\\_19\\_20.pdf](https://www.ufop.de/files/7515/7797/1943/WEB_UFOP_Global_Supply_Report_A5_EN_19_20.pdf).
- Veza, I., Afzal, A., Mujtaba, M. A., Tuan Hoang, A., Balasubramanian, D., Sekar, M., Fattah, I. M. R., Soudagar, M. E. M., El-Seesy, I., Djamari, D. W., Hananto, A. L., Putra, N. R., & Tamaldin, N. (2022). Review of artificial neural networks for gasoline, diesel and homogeneous charge compression ignition engine. *Alexandria Engineering Journal*, 61(11), 8363–8391. <https://doi.org/10.1016/j.aej.2022.01.072>
- Warner, J. D., & Lewis, A. K. (2019). Evaluation of the risks of contaminating low erucic acid rapeseed with high erucic rapeseed and identification of mitigation strategies. *Agriculture*. <https://doi.org/10.3390/agriculture9090190>
- Zhou, L. (2013). *Reaction kinetics of biodiesel production by using low quality feedstock*. Master of Applied Science, University of Regina, Saskatchewan, Canada.

## Authors and Affiliations

**M. A. Hazrat<sup>1</sup> · M. G. Rasul<sup>1</sup> · M. M. K. Khan<sup>2</sup> · N. Ashwath<sup>3</sup> · I. M. R. Fattah<sup>4,5</sup>  · Hwai Chyuan Ong<sup>6</sup> · T. M. I. Mahlia<sup>7</sup>**

- <sup>1</sup> School of Engineering and Technology, CQUniversity Australia, Rockhampton, QLD 4701, Australia
- <sup>2</sup> School of Engineering and Technology, CQUniversity Australia, Melbourne, VIC 3000, Australia
- <sup>3</sup> School of Health, Medical and Applied Sciences, CQUniversity Australia, Rockhampton, QLD 4701, Australia
- <sup>4</sup> Centre for Technology in Water and Wastewater (CTWW), School of Civil and Environmental Engineering, University of Technology Sydney, Ultimo, NSW 2007, Australia
- <sup>5</sup> Department of Mechanical Engineering, College of Engineering, Universiti Tenaga Nasional, Kajang 43000, Selangor Darul Ihsan, Malaysia
- <sup>6</sup> Future Technology Research Center, National Yunlin University of Science and Technology, Douliou, Taiwan
- <sup>7</sup> Centre for Green Technology (CGT), School of Civil and Environmental Engineering, University of Technology Sydney, Ultimo, NSW 2007, Australia